

# DOSY NMR Studies of Chemical Exchange Behavior of Poly(2-hydroxyethyl methacrylate)

Ronda Plummer, David J. T. Hill, and Andrew K. Whittaker\*

Centre for Magnetic Resonance and Australian Institute for Bioengineering and Nanotechnology,  
University of Queensland, QLD 4072, Australia

Received February 16, 2006; Revised Manuscript Received March 21, 2006

**ABSTRACT:** PFG-NMR was used to study the chemical exchange of linear PHEMA having a range of molecular weights with water in DMSO containing varying quantities of water. The aim was to investigate the use of PFG-NMR to study chemical exchange between a polymer with exchangeable protons and a small fast diffusing molecule to provide insight into the conformation adopted by a polymer in solution. The experimental data were simulated closely for the two-site exchange case using the Bloch equations modified for chemical exchange and diffusion. The exchange rate could be used to detect changes in polymer conformation resulting from changes in the solvent. PHEMA of MW 10 000 showed significant time-dependent changes in exchange rate, resulting from preferential solvation of the OH sites by water, and subsequent conformational changes which altered accessibility of the OH sites to water. This behavior was not observed for larger MW PHEMA, which adopted a stable conformation immediately. Large changes in the exchange rate were not reflected in changes to the hydrodynamic radius, suggesting that a minimal *overall* change in the chain dimensions occurred. DMSO was found to be a poor solvent for PHEMA, which adopts a compact conformation in DMSO. This work has demonstrated that PFG-NMR is a sensitive method for detecting subtle changes in polymer conformation in polymers with exchangeable protons.

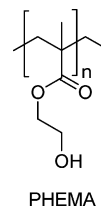
The recent advent of facile routes to well-defined polymer architectures is leading to a renewed focus on methods of polymer characterization. Since a large focus of the synthetic effort is toward polymers for use in the human body, an important field of endeavor will be the development of methods for measurement of the interaction of small molecules with polymers.

PFG-NMR spectroscopy is a well-established, reliable method for obtaining diffusion coefficients of molecules or complexes in solution. Interactions between a particular molecule and the components of a solution will influence the diffusion coefficient measured for that molecule; high-resolution PFG-NMR experiments can therefore provide detailed information about intermolecular interactions in solution.<sup>1</sup> Applications include the analysis of polymer mixtures,<sup>2</sup> affinity/binding studies,<sup>3</sup> and the study of chemical exchange.<sup>1</sup> These experiments are usually referred to as diffusion-ordered spectroscopy (DOSY); the components of a mixture are separated as a function of their respective diffusion coefficients.<sup>1,4</sup> The data can be displayed as a pseudo-2D NMR spectrum with chemical shifts in one dimension and diffusion coefficients in the other.

The measurement of chemical exchange can provide insight into the conformational and dynamic characteristics of a macromolecule,<sup>5</sup> and numerous NMR experiments have been developed to measure this property, e.g., exchange spectroscopy (EXSY),<sup>6</sup> time-resolved measurements in D<sub>2</sub>O, and PFG-NMR methods.<sup>5</sup> It has been demonstrated that PFG-NMR can be used to provide information on exchange rates for systems in fast or slow exchange with respect to chemical shift.<sup>8–11</sup> Slow exchange in chemical shift refers to an NMR spectrum in which the two exchanging components are resolved in chemical shift; fast exchange in chemical shift describes the situation where a population-weighted average signal is observed. Moonen et al.<sup>9</sup>

originally explored the concept that a proton exchanging between sites on two different molecules with unequal diffusion coefficients would exhibit a diffusion coefficient between the two values at the fast exchange limit in diffusion. The actual value observed would be a population-weighted average of the lifetimes in the two states. In the limit of slow exchange in diffusion, the diffusion coefficients would be those observed in the absence of exchange. For observations in the diffusion dimension the variable is the square of the gradient area rather than time. Time has an influence in the form of the selected diffusion time, and this parameter can be varied in some cases to observe the fast and slow exchange limits without altering the physical state of the sample.<sup>1</sup>

Poly(2-hydroxyethyl methacrylate) (PHEMA) is a hydrogel widely used in biomedical applications since 1960.<sup>12–14</sup>



PHEMA is insoluble in water but swells considerably due to the affinity of water for the hydrophilic hydroxyl sites. In a DMSO–water mixture, PHEMA dissolves and the exchangeable proton hydroxyl site and water are well separated in the chemical shift dimension, enabling the individual peak areas to be integrated (see Figure 1). Chemical exchange between the PHEMA OH sites and water can therefore be easily monitored in the diffusion dimension. The large difference between the diffusion coefficients of PHEMA and water means that exchange between these sites will produce a significant effect on the OH signal magnetization decay. In this paper the chemical exchange properties of a series of linear, low polydispersity index (PDI)

\* Corresponding author: Tel +61 7 3365 4100, Fax +61 7 3365 3833, e-mail andrew.whittaker@cmr.uq.edu.au.

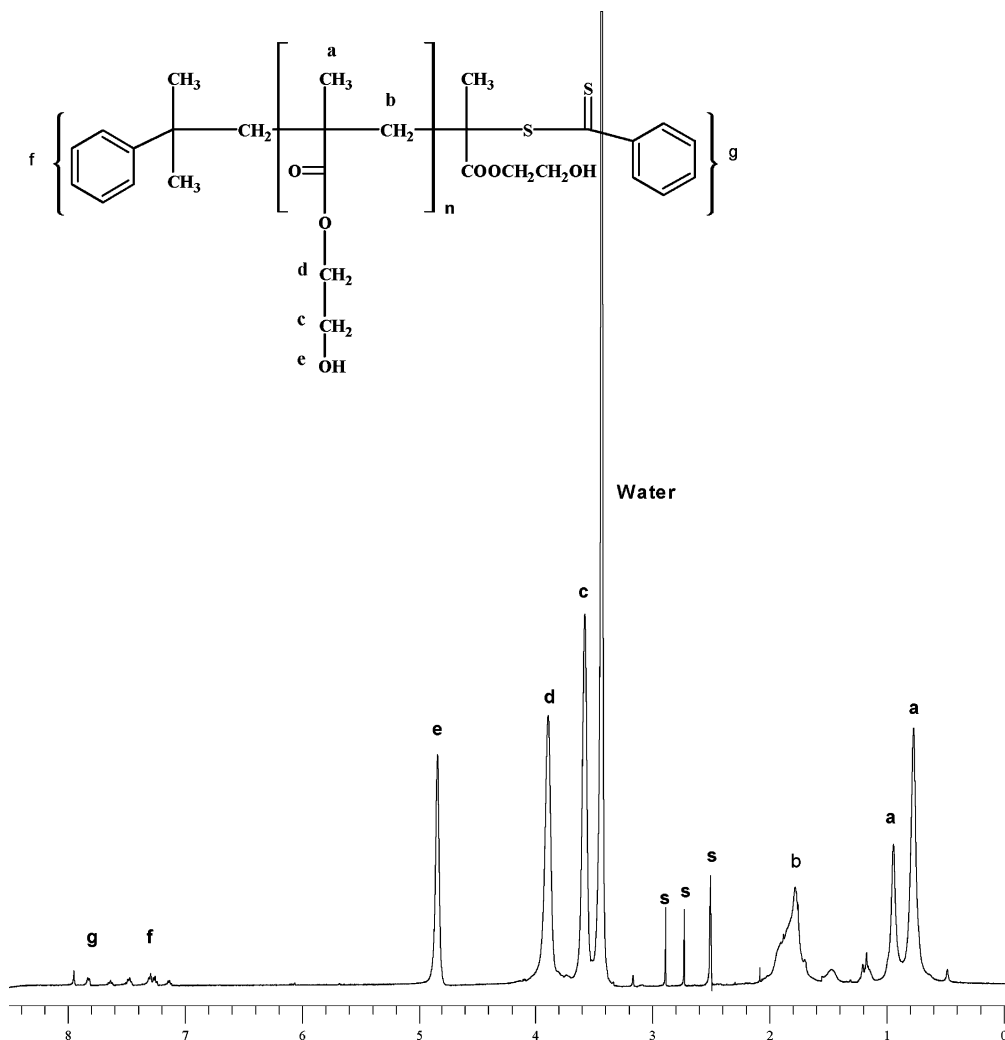


**Figure 1.**  $^1\text{H}$  NMR spectrum of 10K PHEMA in  $\text{DMSO-}d_6$ . Aromatic signals originate from end groups of the RAFT agent cumyl dithiobenzoate.

PHEMA of molecular weight range 10 000–230 000 were studied using PFG-NMR. The PHEMA was dissolved in  $\text{DMSO-}d_6$  containing varying quantities of water to determine the effect of water concentration on the chemical exchange rate.

The aim of this work was to investigate the use of PFG-NMR for the study of chemical exchange between a polymer with exchangeable protons and a small fast diffusing molecule—in this case water. The results show that the method is unusually sensitive to subtle changes in polymer conformation and interactions of the polymer exchangeable sites with water. A range of molecular weights were studied in order to determine the effect of chain length on behavior of PHEMA in solution. The experimental data were simulated using the Bloch equations modified for chemical exchange and diffusion for the case of two-site exchange.<sup>1</sup>

## Experimental Section

**Materials.** All synthetic reagents were analytical grade or higher and used as received unless stated otherwise. HEMA (Aldrich) was distilled under reduced pressure (65 °C, 3.5 mmHg) and stored at –20 °C until use. PHEMA was prepared by reversible addition–fragmentation chain transfer (RAFT) polymerization in *N,N*-dimethylformamide (DMF) using cumyl dithiobenzoate (CDB) as RAFT agent. For example, to prepare a target molecular weight of 10 000, a stock solution of HEMA (2 M), AIBN ( $3.5 \times 10^{-3}$  M), and cumyl dithiobenzoate ( $2.6 \times 10^{-2}$  M) in DMF was prepared. Generally, 0.5 mL aliquots of the stock solution were transferred to 2 mL tubes and deoxygenated by four freeze–evacuate–thaw

cycles and flame-sealed under vacuum. Polymerization was conducted at 60 °C in a constant temperature water bath, and samples removed at regular intervals to determine conversion using FT-NIR. Dried PHEMA was dissolved in a 50:50 methanol/THF mixture followed by precipitation in hexane; this method provided polymers of acceptable purity as determined by  $^1\text{H}$  NMR.

PHEMA was dissolved in  $\text{DMSO-}d_6$  at a concentration of 10  $\text{mg mL}^{-1}$ , and 20, 40, or 60  $\mu\text{L}$  of Millipore water was added using a micropipet. Samples were placed on a shaker for 5 min and then equilibrated for 2 h prior to measurement. All solutions were stored in a tightly sealed jar containing desiccant to prevent changes in the water content of the solutions (storage temperature was 25 °C). Parafilm was used to seal between the NMR tube and cap to prevent moisture being absorbed during experiments.

**NMR Measurements.** All experiments were conducted at 298 K. NMR spectroscopy was carried out using a Bruker Avance DRX 500 spectrometer operating at 500.13 MHz for protons and equipped with a 5 mm triple-resonance ( $^1\text{H}$ ,  $^{13}\text{C}$ ,  $^{15}\text{N}$ )  $z$ -gradient probe equipped with actively shielded gradients. The  $z$ -gradient was calibrated at 298 K with a HDO sample containing 0.1  $\text{mg mL}^{-1}$   $\text{GdCl}_3$ . The maximum  $z$ -gradient amplitude was 50 G/cm. A 90° pulse calibration was performed for each new sample for DOSY experiments. A bipolar pulse longitudinal eddy current delay (BPPLED)<sup>1</sup> pulse sequence or, if convection was a problem, a bipolar pulse pair double stimulated echo pulse sequence (BPPD-STE)<sup>15</sup> pulse sequence was used. The pulse sequences included a 5 ms delay to allow residual eddy currents to decay. Sine-shaped gradient pulses were utilized to further minimize eddy currents. The pulse gradient duration  $\delta$  was chosen for each diffusion time

**Table 1.** Diffusion Coefficients and Molar Ratios of H<sub>2</sub>O:OH for HEMA and 10K PHEMA Solutions

sample	sample code	$D_{\text{H}_2\text{O}} = D_A$ ( $10^{-10} \text{ m}^2 \text{ s}^{-1}$ )	$D_{\text{CH}_3} = D_B$ ( $10^{-11} \text{ m}^2 \text{ s}^{-1}$ )	OH:H <sub>2</sub> O integrated area (NMR)	OH (M)	H <sub>2</sub> O (M)	molar ratio H <sub>2</sub> O:OH
HEMA no added water time = 0 days	HEMA-0	8.2	41.1	1:4	0.077	0.154	2
HEMA 20 $\mu\text{L}$ water added time = 0 days	HEMA-20	8	39.3	1:30	0.077	1.16	15
10K PHEMA no added water time = 0 days	10K-0	7.71	4.19	1:5	0.077	0.194	2.5
10K-0 time = 12 months	10K-0-12M						
10K PHEMA 20 $\mu\text{L}$ added water time = 0 days	10K-20-0D	7.32	4.21	1: 32	0.077	1.23	16
10K PHEMA 20 $\mu\text{L}$ added water time = 21 days	10K-20-21D	7.61	4.14	1: 32	0.077	1.23	16
10K-20-21D time = 6 months	10K-20-6M						
10K PHEMA 40 $\mu\text{L}$ water added to 10K-20-21D time = 0 days	10K-60-21D	7.17	4.02	1:90	0.074	3.34	45

in order to obtain the minimum residual signal for each component at maximum gradient strength. The pulse gradients were incremented from 2 to 95% of the maximum gradient strength in a linear ramp (24 steps). A spectral window of 6000 Hz was accumulated in an acquisition time of 2.7 s. A relaxation delay of  $5T_1$  of the slowest relaxing signal was used (7 s). The FIDs were collected into 16K data points; 16–32 scans and 4 dummy scans were acquired on each sample. Following acquisition the FIDs were Fourier transformed applying zero-filling to 16K data points and an exponential window function with line broadening factor 1–5 Hz.

Data were processed using Bruker XWIN NMR software; the diffusion coefficients were obtained from a single- or double-exponential nonlinear least-squares fitting of the echo attenuation decay. Peak intensities were monitored for all diffusion analyses. The diffusion coefficients for PHEMA were obtained from a single-exponential fit of the echo attenuation decay of the methyl protons, which do not undergo chemical exchange. Diffusion coefficients were obtained by monitoring the signal attenuation as a function of the applied magnetic field gradient amplitude ( $g$ ), and fitting eq 1 or 2 to the results, for monoexponential or biexponential decays, respectively.<sup>16</sup>

$$I = I_0 \exp(-D\gamma^2\delta^2g^2(\Delta - \delta/3)) \quad (1)$$

$$I = I_{0A} \exp(-D_A\gamma^2\delta^2g^2(\Delta - \delta/3)) + I_{0B} \exp(-D_B\gamma^2\delta^2g^2(\Delta - \delta/3)) \quad (2)$$

where  $I$  is the resonance intensity measured for a given gradient amplitude,  $g$ ,  $I_0$  is the signal intensity with no gradient applied,  $\gamma$  is the gyromagnetic ratio,  $\delta$  is the gradient length, and  $\Delta$  is the diffusion time.

**Simulations.** Experimental diffusion curves were simulated using the Bloch equations modified for diffusion and exchange in order to estimate the relative rates of chemical exchange for HEMA and PHEMA. A simulation of the two-site exchange case was compared to the experimental data for the decay of water and hydroxyl signals for the HEMA and PHEMA samples. Values of  $k_A$  and  $k_B$  were varied iteratively to mimic the experimental decay curves in each case. It was assumed that all OH sites were available to exchange in the HEMA system. The monomer was therefore used to characterize the case of unhindered exchange. The simulations of the HEMA data were performed first, and the values of  $k_A$  and  $k_B$  obtained were used as starting values in the simulations of the data for PHEMA in solution.

## Results and Discussion

**Exchange Behavior of HEMA.** As a first experiment the diffusion and exchange behavior of HEMA monomer was measured in order to characterize the exchange behavior of the hydroxyl sites in small molecules. The diffusion coefficients

obtained for HEMA and water in DMSO- $d_6$  and the molar ratios of water to HEMA hydroxyl groups, determined by integration of the  $^1\text{H}$  NMR spectrum, are shown in Table 1. Figure 2 compares the logarithmic normalized hydroxyl signal intensity of HEMA as a function of the squared gradient intensity  $\gamma^2\delta^2g^2 - (\Delta - \delta/3)$  (known as a Stejskal–Tanner plot) for diffusion times,  $\Delta$ , of 50–500 ms. Data for both HEMA-0 (no added water) and HEMA-20 (20  $\mu\text{L}$  of added water) cases are shown. The data for the methyl signal of HEMA are included as a reference for the case of zero chemical exchange. The curves for the hydroxyl signals show excellent linearity for all  $\Delta$  values, indicating fast exchange in the diffusion dimension. The addition of 20  $\mu\text{L}$  of water  $\text{mL}^{-1}$  of DMSO- $d_6$  resulted in a small increase in the slope of the curve for the 500 ms data shown in Figure 2a. The system is close to the fast exchange limit in diffusion, so the addition of extra water would not be expected to result in a significant increase in exchange rate, but rather the small increase observed reflects the increased probability of water molecules encountering a hydroxyl site.

The Stejskal–Tanner plots for both the hydroxyl and water signals of HEMA for  $\Delta$  values of 50 and 500 ms are shown in Figure 2b. The data illustrate that the system is approaching the fast exchange limit in diffusion at 50 ms; at 500 ms both the hydroxyl and water curves coincide, and the population-weighted average diffusion coefficient is observed. At this point the system can be considered to be at the fast exchange limit in diffusion. Because of fast exchange of HEMA hydroxyl groups with water in the diffusion dimension, the slow exchange limit was not observed in the range of diffusion times used for the experiments. The mean residence lifetime of a proton on a hydroxyl site of HEMA can therefore be estimated as  $<50$  ms (the shortest value of  $\Delta$  used), and the exchange rate  $k > 20 \text{ s}^{-1}$ . It is reasonable to assume that the case of HEMA represents the situation where most of the OH sites are exchanging, so HEMA was used as a benchmark to estimate changes in the accessibility of OH sites in the PHEMA polymers reported in the following sections.

**Exchange Behavior of 10 000 MW PHEMA.** Table 2 summarizes the diffusion coefficients of water and 10K PHEMA and the molar ratios of water and hydroxyl groups for the samples of 10K PHEMA in DMSO- $d_6$  solutions. Logarithmic normalized hydroxyl signal intensities of 10K PHEMA as a function of the squared gradient intensity are shown in Figure 3a–d. The intensity of the signal due to the methyl group of PHEMA is shown in each plot to show the behavior in the absence of exchange.

Figure 3a shows the results for 10K-0 where no water was added to the DMSO- $d_6$ , and only the water initially present in

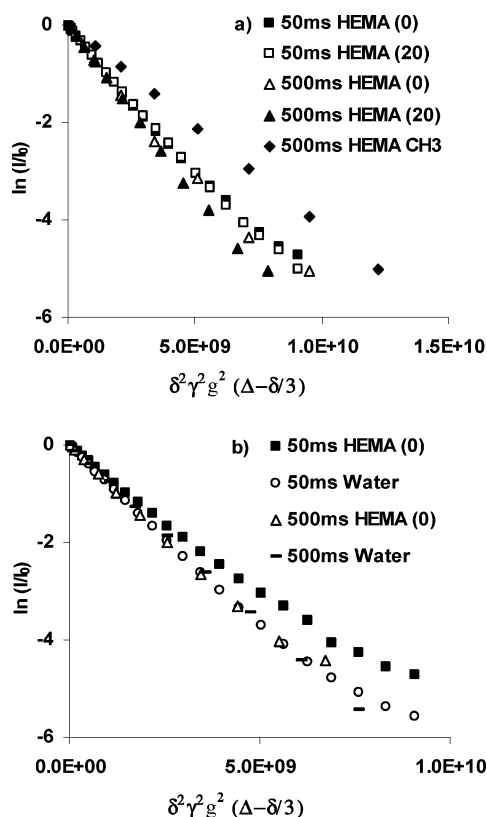


**Figure 2.** Logarithmic normalized signal intensity as a function of  $\gamma^2 \delta^2 g^2 (\Delta - \delta/3)$ . (a) HEMA hydroxyl signals: HEMA-0  $\Delta = 50$  and 500 ms and HEMA-20  $\Delta = 50$  and 500 ms; HEMA CH<sub>3</sub> signal  $\Delta = 500$  ms. (b) HEMA-0  $\Delta = 50$  and 500 ms hydroxyl and water signals.

the polymer/DMSO-*d*<sub>6</sub> is involved in exchange with the polymer hydroxyl groups. In this sample the ratio of water to OH groups is 2.5. In contrast to the plots for HEMA monomer, the decay curves for 10K-0 are obviously biexponential in nature. The rapidly decaying component (fast diffusion) is associated with water diffusion ( $D_A$ ) and the slow diffusing component with the polymer diffusion ( $D_B$ ). The initial slope is  $D = p_A D_A + p_B D_B$ , where  $p_A$  and  $p_B$  are the probability of occupation of site A or B; the slope at high values of gradient strength approaches  $D_B$ .<sup>1</sup> The data in Figure 3a reveal that in the range of values of the diffusion time  $\Delta$  from 50 to 750 ms the system is in the intermediate exchange regime in diffusion; the slow and fast exchange limits are not observed, but the proportion of the slow diffusing component is very small at  $\Delta$  values  $> 200$  ms.

With a diffusion time of 750 ms the system is approaching the fast exchange limit but still exhibits a slight degree of biexponential behavior. The  $T_1$  relaxation times for the PHEMA protons spanned the range 600–1200 ms, so in order to maintain good signal-to-noise ratios for the signals of interest,  $\Delta$  values longer than 750 ms were not used. The slow exchange limit is not observed, so the mean residence time of a proton on a hydroxyl site of PHEMA in the 10K-0 sample can be estimated as  $< 50$  ms, corresponding to an exchange rate  $k$  of  $> 20$  s<sup>-1</sup>.

Figure 3b demonstrates the effect of adding 20  $\mu$ L of water mL<sup>-1</sup> of DMSO-*d*<sub>6</sub> and measuring the exchange behavior of the polymer solution after equilibration for 2–4 h, i.e., 10K-20-0D. The addition of water produces a small change in the exchange properties; there appears to be slower exchange occurring for a given diffusion time compared with the case for 10K-0, but an exchange rate  $k$  of  $> 20$  s<sup>-1</sup> can only be estimated since the slow exchange limit is not observed.

The data in Figure 3c show the results for the same sample stored for a period of 21 days: 10K-20-21D. The sample was

stored in a desiccator, so the amount of additional water absorbed over this time period was negligible (see Table 1). In this case there is a dramatic decrease in the rate or number of sites undergoing exchange compared with the freshly prepared sample. The slopes of all of the curves are very similar to that for the nonexchanging methyl signal, indicating very slow or negligible exchange is occurring. The mean residence time of protons on hydroxyl sites of 10K-20-21D can still only be estimated as  $< 50$  ms, or an exchange rate  $k$  of  $> 20$  s<sup>-1</sup>. This is because at a diffusion time of 50 ms the curve is quite linear, but the diffusion coefficient extracted from this curve is still larger than  $D_{CH_3}$ , indicating that the slow exchange limit has not been attained. Figure 3d shows the effect of adding 40  $\mu$ L of extra water to the 10K-20-21D sample; the exchange properties of the 10K-60-21D sample returned to levels similar to the freshly prepared sample containing 20  $\mu$ L of added water mL<sup>-1</sup> of DMSO-*d*<sub>6</sub>.

The exchange behavior observed for the 10K PHEMA samples with added water is very different to that observed for the monomer. The addition of water resulted in a small increase in the exchange rate for HEMA monomer, which is expected given the higher probability of an exchange encounter, but caused a *decrease* in the exchange rate for PHEMA. The addition of water is either causing a change in the conformation of the polymer or affecting the interactions of the OH sites with water. Furthermore, the effect is time dependent. The 10K-0 sample shows similar behavior to the HEMA-0 sample, and the exchange properties do not change with time. This indicates that a large proportion of 10K-0 OH sites are exchanging with water and that the sample rapidly equilibrates and remains stable.

The Stejskal–Tanner plots for the water signal in each of the 10K PHEMA samples are shown in Figure 4a,b for diffusion times  $\Delta = 50$  and 200 ms. The data illustrate that the amount of slow diffusing component resulting from exchange with the polymer hydroxyl sites is very small, i.e.,  $p_B$  is low. This is a result of the large number of water molecules relative to OH sites; only a small percentage of the total water pool is involved in exchange with polymer OH sites. The 10K-0 sample contains the least amount of water, and the intensity of the slow diffusing component is therefore highest in this sample. As expected, the proportion of the slow diffusing component in the 10K-20-0D and 10K-20-21D samples is much smaller than for 10K-0, but the 10K-60-21D sample has a higher proportion of the slow diffusing component than 10K-20-0D or 10K-20-21D. This is surprising considering that 10K-60-21D contains the largest amount of water; this may be due to experimental error, since signal-to-noise is poorest at high gradient, or could reflect interactions between fast and slow diffusing water (discussed later).

Analysis of the Stejskal–Tanner plots for the water signal can be misleading because of the possibility of H<sub>2</sub>O–H<sub>2</sub>O exchange following OH–H<sub>2</sub>O exchange during the diffusion time. This type of exchange is more likely as the concentration of water increases. It is detected as a decrease in the amount of slow diffusing component with increasing  $\Delta$  (compare parts a and b of Figure 4); the opposite behavior would be expected if only OH:H<sub>2</sub>O exchange were possible. It is therefore difficult to compare the water decay curves of the different samples, since the amount of H<sub>2</sub>O–H<sub>2</sub>O exchange will vary between samples containing different quantities of water.

An exchange rate  $k > 20$  s<sup>-1</sup> was estimated for all the 10K PHEMA samples discussed above, but it is obvious from Figure 3 that the amount of exchange varied considerably under the different solvent conditions. Unlike HEMA monomer, the



**Table 2. Comparison of  $k_B$  Values and % Exchanging Sites Obtained Using Graphical Analysis and Simulations for HEMA and 10K PHEMA Samples**

	sample	$k_B$ ( $s^{-1}$ ) graph	$k_B$ ( $s^{-1}$ ) simulation	$k_B$ ( $s^{-1}$ ) mean <sup>a</sup>	$\tau_B$ (s) mean <sup>a</sup>	% exchanging OH sites graphical	% exchanging OH sites relative to HEMA
1	HEMA-0		20		0.05		100
2	HEMA-20		25		0.04		100
3	10K-0	11.7	14	12.9	0.078	63	64
4	10K-20-0D	7.1	10	8.6	0.116	32	34
5	10K-20-21D	0.96	1	0.98	1.02	3.2	4
6	10K-60-21D	6.9	9	7.95	0.126	14	32
7	10K-0-12M	7.6	10.5	9.1	0.11		36
8	10K-20-6M		25	25	0.04		100

<sup>a</sup> Mean of the  $k_B$  and  $\tau_B$  values obtained for graph and simulation.

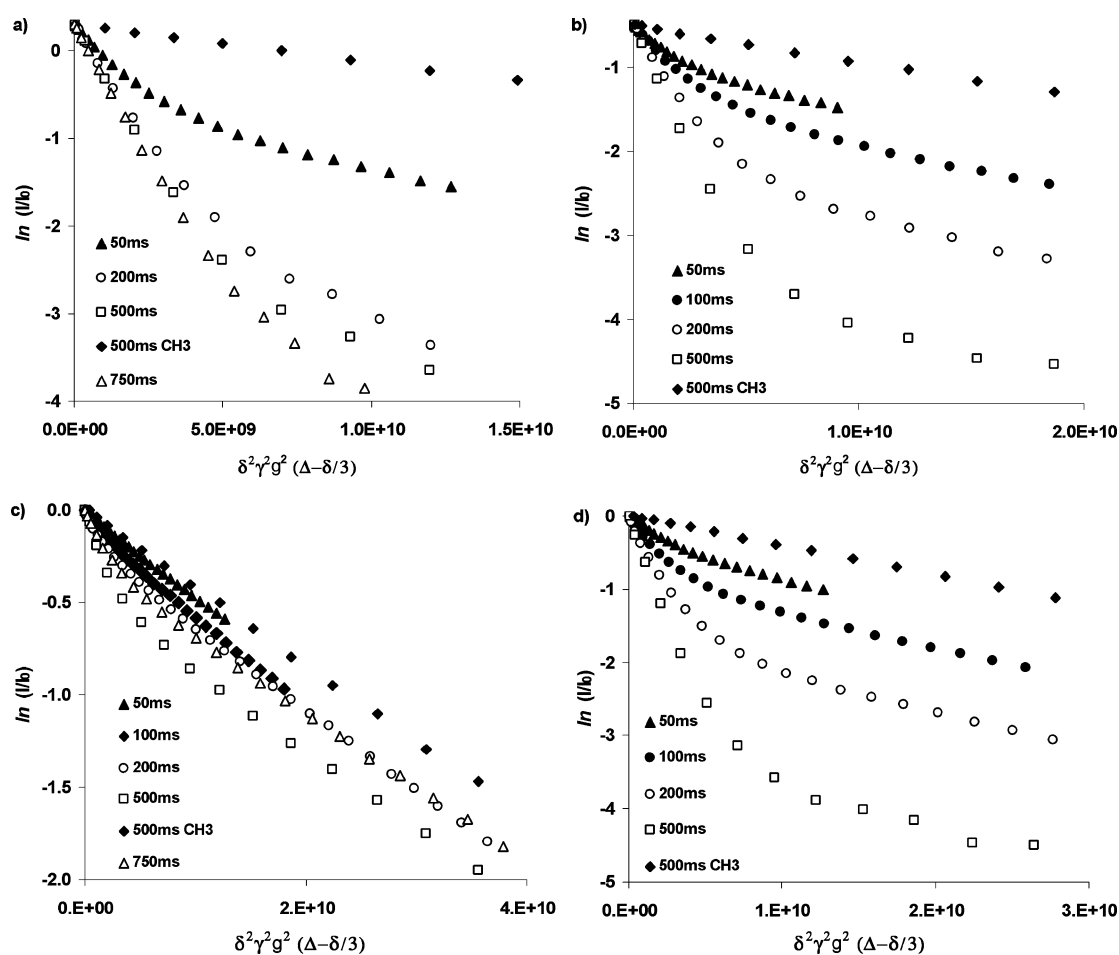


**Figure 3.** Logarithmic normalized signal intensity as a function of  $\gamma^2 \delta^2 g^2 (\Delta - \delta/3)$ : (a) 10K-0 hydroxyl signals  $\Delta = 50$ –750 ms; (b) 10K-20-0D  $\Delta = 50$ –750 ms; (c) 10K-20-21D  $\Delta = 50$ –750 ms; (d) 10K-20-21D after addition of 40  $\mu$ L of  $H_2O$ . PHEMA  $CH_3$  signal  $\Delta = 500$  ms shown for each sample as reference for the zero exchange case.

polymer hydroxyl sites will be in a range of different environments, so a distribution of exchange rates is expected. Even at short values of the diffusion time  $\Delta$  the fastest exchanging protons will still be detected, and the observed signal attenuation will be biexponential. Therefore, when the slow exchange limit is not observed, estimates of  $k$  obtained from inspection of Stejskal–Tanner plots will be less accurate. If relative changes are to be detected, however, comparison of the Stejskal–Tanner plots is sufficient to detect changes in macromolecular behavior as demonstrated for 10K PHEMA.

**More Accurate Estimation of the Exchange Rate.** The point of intersection of the asymptote characterizing the slow diffusing component and the ordinate ( $\ln(\text{intensity}) = \exp(-\Delta/\tau_B)$ ) corresponds to the fraction of nonexchanging protons (for which  $1/\tau_B = k_B$ ).<sup>17</sup> A plot of  $\ln(\text{slow intensity})$  vs diffusion time  $\Delta$  has a linear dependency, so if data are obtained using a

range of  $\Delta$  values, linear regression gives the value of the nonexchanging population (intercept) and the value of  $k_B$  (slope).<sup>12</sup> This type of analysis only works for situations where the exchange is intermediate/slow because otherwise there is a large error in the intensity of the slow diffusing component.

It should also be possible to simulate the experimental diffusion curves using the Bloch equations modified for diffusion and exchange<sup>1</sup> in order to estimate the relative rates of chemical exchange for HEMA and PHEMA. The results could then be compared with the values obtained using the graphical method. The experimental decay curves for the water and hydroxyl signals of HEMA and PHEMA samples were simulated for the two-site exchange case using the modified Bloch equations, as described in the Experimental Section. The values of the exchanging population were obtained by comparing the exchange rates of the polymer to the average value

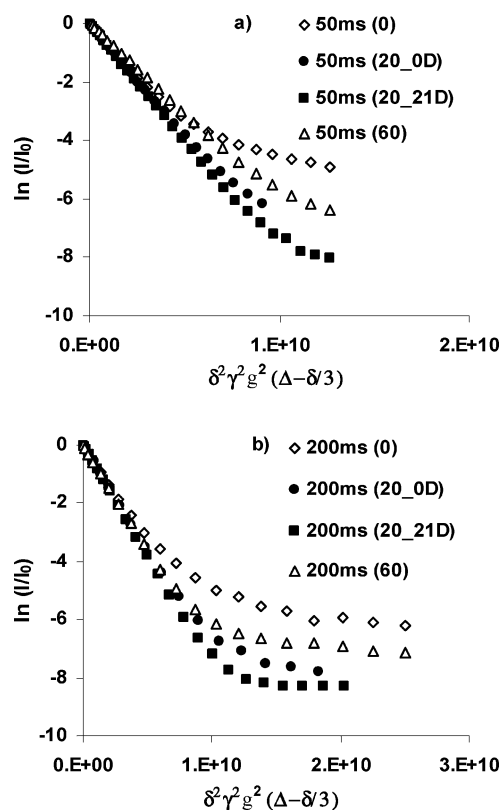


**Figure 4.** Logarithmic normalized water signal intensity as a function of  $\gamma^2 \delta^2 g^2 (\Delta - \delta/3)$ : (a) 10K-0, 10K-20-0D, 10K-20-21D, and 10K-60-21D water signals  $\Delta = 50$  ms; (b) 10K-0, 10K-20-0D, 10K-20-21D, and 10K-60-21D water signals  $\Delta = 200$  ms.

obtained for HEMA. The values of  $k_B$  obtained from simulations of experimental attenuation curves at different values of the diffusion time  $\Delta$  were very consistent for  $\Delta > 200$  ms; the average values are listed in Table 2. Analysis of the data acquired using short values of the diffusion time  $\Delta$  produced variable results due to the short observation time relative to the rates of exchange—these values were not included.

A representative example is shown for each sample in Figure 5a–f; the simulated data for the case of no exchange ( $k_A$  and  $k_B \rightarrow 0$ ) are included for reference. The experimental data are simulated quite closely using the two-site exchange model; plots of the residuals of each fit gave very similar trends to those obtained by fitting the experimental data using the Bruker diffusion software. The estimated exchange rates obtained using the graphical method and data simulations are compared in Table 2, entries 1–6.

The values of  $k_B$  obtained from the simulations for 10K PHEMA are in good agreement with the values measured using graphical analysis. The values obtained for the exchanging populations are also very similar using either method; the only discrepancy was the value obtained for the sample containing 60  $\mu$ L of water. The monomer undergoes the fastest exchange as expected, and the rate increased by around 20% when 20  $\mu$ L of water was added to the sample. The 10K-0 sample has the highest proportion of exchanging sites among the polymers, estimated to be 63–64% relative to HEMA. Not all potentially exchangeable sites on a polymer necessarily participate in chemical exchange because they may be inaccessible to solvent due to the folded or partially collapsed conformation adopted by the polymer. Also, it is expected that a distribution of exchange rates would exist due to varying accessibility of solvent to the exchanging sites; the calculated value is therefore an average. The mean  $k_B$  value obtained for the PHEMA

samples was somewhat smaller than the original estimate of  $>20$  s $^{-1}$  obtained from inspection of the Stejskal–Tanner plots. The addition of water causes a decrease in the number of exchanging sites which is reflected in a reduction of the exchange rate to 8.6 s $^{-1}$  for 10K-20-0D. After 21 days the sample containing 20  $\mu$ L of added water has only 3–4% of sites undergoing exchange; the apparent exchange rate has reduced dramatically, suggesting most of the hydroxyl sites are inaccessible to water molecules. Addition of a further 40  $\mu$ L of water to the 21-day sample then produces an increase in the hydroxyl exchange rate to a value similar to that observed when the water was first added.

**Long-Term Changes in Chemical Exchange Properties of 10K PHEMA Samples.** The exchange properties of the 10K-20-21D and the 10K-0 samples were measured again after 6- and 12-month storage periods. The values of  $k_B$  obtained for the stored samples are compared with the original values in Table 2. In the case of the 10K-20-21D sample, a vast increase in the rate of exchange occurred after 6 months (entry 8 Table 2); the exchange rate became similar to HEMA and was much faster than 10K-0. No further change occurred after a total storage time of 12 months. The amount of water in the 10K-20-21D sample increased from an OH:H<sub>2</sub>O ratio of 1:32 to 1:45 after 6 months and to 1:60 after 12 months, even though the storage vessel contained desiccant. The 10K-0 sample was also measured after a 12-month storage period (entry 7, Table 2) and had also absorbed water. The OH:H<sub>2</sub>O ratio had increased from 1:5 to 1:30; the exchange rate for this sample was slightly less than when freshly prepared and similar to the 10K-20-0D sample which contained a similar amount of water (see Table 1). The  $^1$ H NMR spectra of all the stored samples were carefully examined for evidence of polymer degradation, and none could be detected.

It appears that over an extended time period the polymer conformation changes to form a structure which enables practically all of the OH sites to exchange with water. Since the exchange rate of 10K-20-6M became very similar to the exchange rate obtained for HEMA, close to 100% of available OH sites must be exchanging. The 10K-0-12M sample must be in an intermediate stage of conformational change; a certain water concentration and time period may be necessary to reach a conformation similar to 10K-20-6M. These aspects are discussed in more detail below.

$^1$ H NMR spectra of the 10K-0-12M and 10K-20-6M samples revealed a significant broadening of the OH signal (data not shown). Initially, it was thought that cross-linking of the polymer chains had occurred, though peak area integration showed the expected ratios for all signals. The other polymer signals were unaffected by broadening; the side-chain CH<sub>2</sub> signal closest to the OH site was overlapped by the large water peak, so it was difficult to detect whether this signal was affected. The broadening of the OH signal indicates a shorter  $T_2$  relaxation time for the OH spins and may reflect reduced flexibility of the PHEMA side chain in the vicinity of the OH site.

**A Model for the Observed Behavior.** The significant sensitivity of the exchange behavior of the 10K PHEMA samples to changes in the water concentration and with time suggests that changes in polymer conformation and the details of the interaction of hydroxyl sites with water are occurring. The existence of “bound” water is a well-known phenomenon with polymer hydrogels such as PHEMA and has been detected using a variety of methods, including DSC, NMR relaxation measurements, and small molecular probes.<sup>18–20</sup> It is generally accepted that water initially binds to the most polar hydrophilic

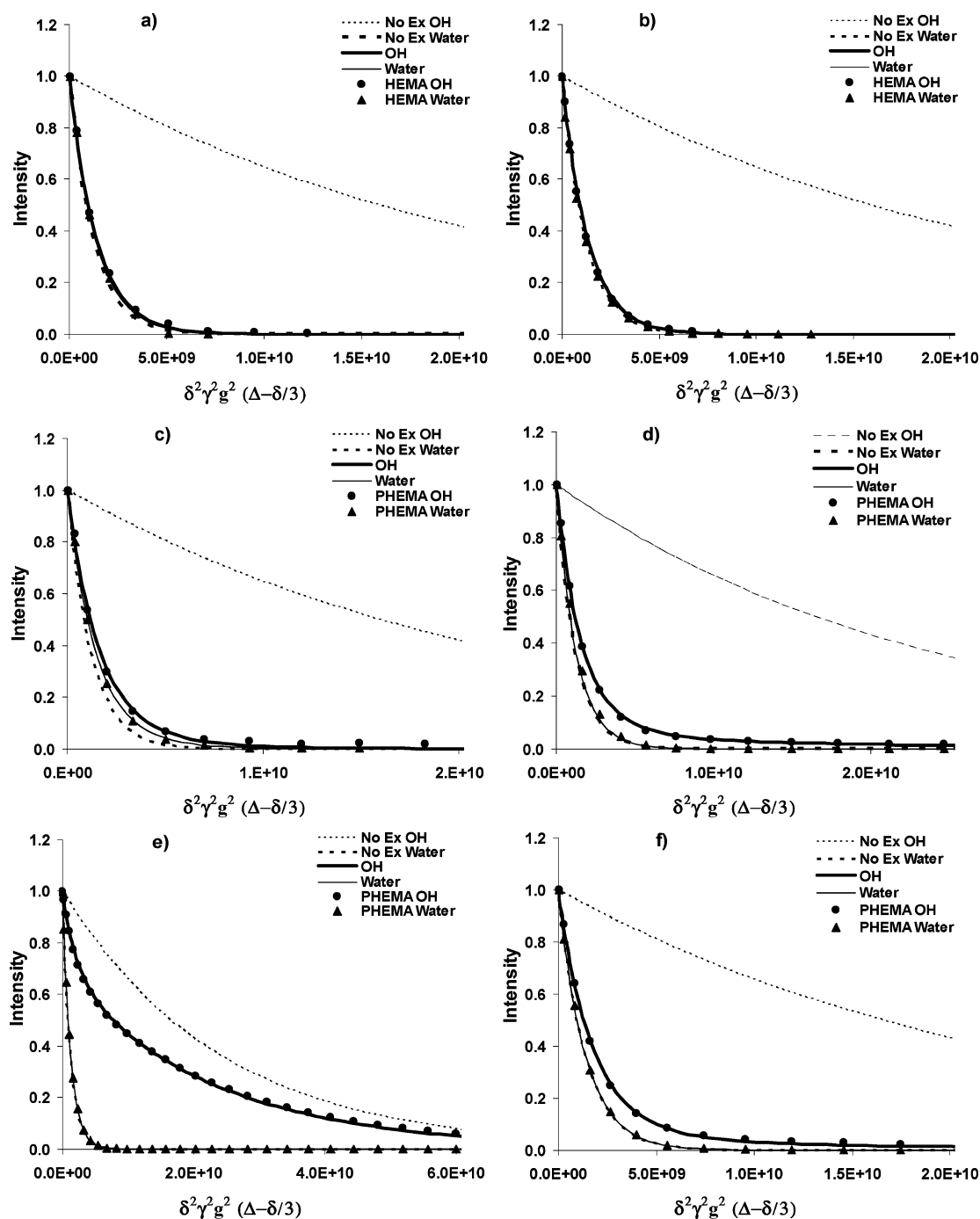


**Figure 5.** Simulations of experimental data using the Bloch equations modified for diffusion and exchange. Experimental OH and water signals, simulated OH and water signals, OH and water signals for the case of zero exchange, and  $k_A$  and  $k_B$  values obtained are shown on each plot. (a) HEMA-0  $\Delta = 500$  ms; (b) HEMA-20  $\Delta = 500$  ms; (c) 10K-0  $\Delta = 400$  ms; (d) 10K-20-0D  $\Delta = 400$  ms; (e) 10K-20-21D  $\Delta = 400$  ms; (f) 10K-60-21D  $\Delta = 400$  ms.

sites (primary bound water) and then interacts with the hydrophobic polymer backbone (secondary bound water).<sup>18</sup> If water molecules become bound to a hydroxyl site as a result of strong hydrogen bonding, a water layer of reduced mobility could be formed, and the apparent diffusion coefficient of water diffusing within the layer would be less than the bulk water. Such behavior has been observed in aqueous solutions of the disaccharide trehalose.<sup>21</sup> The apparent rate of exchange between OH sites and bound water would be reduced compared with exchange involving freely diffusing water; the significant decrease in the exchange rate of 10K-20-21D may reflect a situation similar to this.

Water must have an affinity for the hydroxyl sites of PHEMA because exchange is fast when no water is added to the polymer DMSO- $d_6$  solution, even though the molar ratio  $H_2O:DMSO$  is  $\approx 1:67$ . The water may therefore preferentially solvate the hydroxyl groups of PHEMA, forming a water-rich phase in the vicinity of the polymer. Preferential solvation by one solvent in mixed solvent systems has been reported for a number of polymers.<sup>22–24</sup> Differences in affinity of each solvent for the polymer lead to variation in the composition of the mixed solvent in proximity to the polymer.<sup>23</sup>

If exchange between polymer OH sites and bound/slow diffusing water is to affect the apparent exchange rate, a water

Table 3. Hydrodynamic Radii for Corrected Values of  $D_{CH_3}$  for 10K PHEMA Samples

sample	$D_{CH_3}$ ( $10^{-11}$ m <sup>2</sup> s <sup>-1</sup> )	$D_{DMSO}$ ( $10^{-10}$ m <sup>2</sup> s <sup>-1</sup> )	$D_{CH_3}$ ( $10^{-11}$ m <sup>2</sup> s <sup>-1</sup> ) corrected	$R_H$ ( $10^{-9}$ m)	% change $R_H$	% vol change
10K-0	4.16	6.07	4.16	2.62		
10K-20-0D	4.06	5.81	4.24	2.57	-1.9	-5.6
10K-20-21D	4.18	6.02	4.22	2.59	-1.1	-3.4
10K-60-21D	3.84	5.49	4.25	2.57	-1.9	-5.6
10K-20-6M	3.96	6.11	3.92	2.78	+6.1	19.5
10K-0-12M	3.97	6.13	3.93	2.78	+6.1	19.5

molecule must remain in the slow diffusing water layer for most of the diffusion period. Proton NMR experiments have shown that exchange of water between free and bound states for hydrogels is very fast, i.e., one H<sub>2</sub>O molecule every  $10^{-9}$  s.<sup>18</sup> The system under study here is DMSO containing a small quantity of water, so the solution behavior may be very different. DMSO–water systems show a number of unusual interactions, which are not yet completely understood.<sup>25,26</sup>

If significant numbers of slow diffusing water molecules exist as a layer around the polymer—and do not exchange rapidly with freely diffusing water on the diffusion time scale—the water signal magnetization decay should reflect the larger contribution of the slow diffusing component. As discussed earlier, it is difficult to detect the effect of exchange on the water decay curves because of the large excess of free water and the possibility of H<sub>2</sub>O–H<sub>2</sub>O exchange. A significant slow diffusing component was not observed in the water decay curves for the stored samples (data not shown).

A change in polymer conformation could also cause a reduction in the exchange rate of PHEMA samples with added water. PHEMA swells in water but is not water-soluble;<sup>27</sup> the addition of water to the DMSO would make the solvent poorer and result in OH–H<sub>2</sub>O and C=O–H<sub>2</sub>O bonds being broken and the formation of OH–OH or OH–C=O bonds. The result would be a decrease in the exchange rate because of reduced access of water to exchangeable sites on the polymer.

The 10K-0 sample undergoes relatively fast exchange compared with HEMA and therefore does not fit the bound water scenario described above. The 10K-0 exchange properties are also stable for long periods as long as the water concentration does not change significantly. It is only after addition of 20  $\mu$ L of water and a period of 21 days that the exchange properties are significantly changed. This suggests that if a bound/slow diffusing water layer forms in the vicinity of the polymer as a result of preferential solvation, the process is quite slow. In the presence of added water the polymer must adopt a conformation where access of bulk water to the slow diffusing layer around the OH sites is restricted. The 10K-0 chain conformation may be more expanded because DMSO without added water is a better solvent, so if a bound/slow diffusing layer does form in this sample, access of bulk water is not restricted. It is also possible that a certain concentration of water is required before a slow diffusing or bound water layer can form. It has been calculated that the average number of water molecules that bind to each hydroxyl site on a PHEMA hydrogel is  $\sim 4$ .<sup>20,28</sup> In the case of the sample with no water added there may be insufficient numbers of water molecules to form a stable slow diffusing layer (via a hydrogen-bonding network), so the water diffuses as free water, and the fast exchange between OH and water sites produces an average diffusion coefficient for the exchanging spins. The vast increase in OH exchange rate of the 10K-20-6M sample could indicate that more water molecules are “locked in” around the OH sites; this may force a conformational change to occur which permits rapid exchange between bound/slow diffusing water and freely diffusing water.

To clarify whether a hydration layer or conformational change affected the hydrodynamic properties of the polymer, the  $D_{CH_3}$  was corrected for the effects of viscosity by monitoring the diffusion coefficient of residual DMSO in DMSO-*d*<sub>6</sub>. The  $D_{DMSO}$  obtained for the PHEMA with no added water was used to correct for changes in the viscosity of the polymer solutions containing added water. Once the corrected values were obtained, the hydrodynamic radius of the polymer for each of the solutions was calculated using the Stokes–Einstein relation:<sup>16</sup>

$$D = kT/(6\pi\eta R_H) \quad (3)$$

Here  $k$  is the Boltzmann constant,  $T$  is the temperature,  $\eta$  is solution viscosity, and  $R_H$  is the hydrodynamic radius (for the simple case of a spherical particle).

The hydrodynamic radii calculated from the corrected diffusion coefficients are shown in Table 3. No significant changes in  $R_H$  were observed for the 10K-0, 10K-20-0D, 10K-20-21D, or 10K-60-21D samples. The small volume changes observed even with large changes in the exchange properties of these 10K PHEMA samples suggest that a change in the accessibility of the OH sites involves relatively small changes in chain conformation or that conformational rearrangements can occur with minimal *overall* change in the chain dimensions. The samples stored for periods of 6 and 12 months showed a 6% increase in radius, corresponding to a 19.5% increase in volume. As mentioned earlier, after 6–12 months the polymer OH sites may be preferentially solvated by water, resulting in an expanded conformation where most of the OH sites are exposed to the solvent. The 10K-20-6M and 10K-0-12M samples are the same size, even though the apparent exchange rate of 10K-0-12M is lower than 10K-20-6M and has even decreased slightly relative to 10K-0. The volume increase for 10K-0-12M of around 20% with only a slight change in exchange rate may indicate that insufficient water is present to preferentially solvate enough OH sites to force the polymer to adopt a conformation where all OH sites are accessible.

Solutions of DMSO–water have been shown to exhibit unusual behavior; both thermodynamic and transport properties of DMSO–water solutions have demonstrated that a strong intermolecular attraction exists between the two compounds.<sup>26</sup> The addition of water to liquid DMSO has been shown to result in a decrease in the diffusion coefficient of DMSO; the addition of DMSO to pure water also produced a decrease in the diffusion coefficient of water.<sup>26</sup> Strong hydrogen bonding is believed to be the cause of the decreased mobility of DMSO and water in mixtures of the two solvents. Water–DMSO hydrogen bonds have been shown to be stronger than water–water hydrogen bonds and are thus more difficult to break.<sup>30</sup> Self-diffusion coefficients for both DMSO-*d*<sub>6</sub> and water in the 10K PHEMA solutions are shown in Table 4. It is clear that  $D_{DMSO}$  and  $D_{H_2O}$  are initially decreased upon addition of 20  $\mu$ L of water but *increase* once again after 21 days; another decrease occurs upon addition of a further 40  $\mu$ L of water.  $D_{DMSO}$  and  $D_{H_2O}$  are further



**Table 4. Diffusion Coefficients of Residual DMSO in DMSO-*d*<sub>6</sub> and Water in 10K PHEMA Samples**

sample	$D_{\text{DMSO}}$ ( $10^{-10} \text{ m}^2 \text{ s}^{-1}$ )	$D_{\text{H}_2\text{O}}$ ( $10^{-10} \text{ m}^2 \text{ s}^{-1}$ )
10K-0	6.07	7.71
10K-0-12M	6.13	7.42
10K-20-0D	5.81	7.32
10K-20-21D	6.02	7.61
10K-60-21D	5.49	7.17
10K-20-6M	6.11	7.63

increased in the 10K-20-21D sample after 6 months storage. This behavior supports the concept that a water-rich phase forms around the polymer as a result of preferential solvation of the hydrophilic OH sites by water. The 10K-0 sample has a low amount of water, and it appears that preferential solvation of the OH sites occurs rapidly. Addition of 20  $\mu\text{L}$  of water causes DMSO and water diffusion coefficients to decrease due to formation of strong intermolecular attractions between the two solvents. After 21 days a significant fraction of the water has migrated to preferentially solvate the polymer, and  $D_{\text{DMSO}}$  and  $D_{\text{H}_2\text{O}}$  increase. Addition of 40  $\mu\text{L}$  of extra water disrupts the water-rich phase, and the formation of strong DMSO–water interactions causes  $D_{\text{DMSO}}$  and  $D_{\text{H}_2\text{O}}$  to decrease again. After 6 months, the 10K-20-21D sample shows a further increase in  $D_{\text{DMSO}}$  and  $D_{\text{H}_2\text{O}}$  to values similar to the 10K-0 sample. This indicates practically all of the water is preferentially solvating the polymer at this stage. Combined with the chemical exchange data, the behavior observed for the 10K PHEMA solutions could be interpreted as follows:

**10K-0.** The polymer–solvent interactions are strong, the polymer chain is relatively expanded, and an estimated 63% of OH sites are exchanging. Water preferentially solvates the polymer OH sites and may be bound to the OH sites but is able to exchange freely with water within the DMSO solution (bulk water).

**10K-20-0D.** Initially, the addition of 20  $\mu\text{L}$  of water reduces the goodness of the solvent; polymer–polymer interactions increase, and a conformational rearrangement of the polymer chain occurs to decrease the accessibility of the OH sites to water. There is a corresponding small decrease in  $R_{\text{H}}$ . Access to polymer OH sites is reduced, and a 33% decrease in the rate of OH exchange is observed relative to 10K-0.  $D_{\text{DMSO}}$  and  $D_{\text{H}_2\text{O}}$  decrease, indicating the water is interacting with DMSO, and preferential solvation of PHEMA by water has not yet occurred.

**10K-20-21D.** A slower conformational change as a response to binding of water molecules to OH sites occurs with time; water preferentially solvates the OH sites, and a water-rich solvent phase is formed in the vicinity of the polymer. This is reflected in the increase in  $D_{\text{DMSO}}$  and  $D_{\text{H}_2\text{O}}$ , indicating weaker interactions between the two solvents. The apparent rate of exchange of the OH sites is very low, indicating that exchange of slow diffusing or bound water with the bulk water is slow on the diffusion time scale. An 88% decrease in the rate of exchange is observed relative to 10K-20-0D. This may reflect the polymer conformation adopted at this stage; water is preferentially solvating the OH sites, and this forces the chain

to rearrange in order to minimize interactions between the hydrophilic water-bound OH sites and the hydrophobic polymer backbone. The resulting conformation may restrict access of bulk water to the OH sites, and exchange of bound and bulk water would therefore be slow on the scale of the diffusion time. There is no detected increase in the  $R_{\text{H}}$  compared with the 10K-20-0D sample (see Table 3), but as discussed above, this does not mean that no change in conformation has occurred.

**10K-60-21D.** Addition of 40  $\mu\text{L}$  of water to the 10K-20-21D sample produces a decrease in  $D_{\text{DMSO}}$  and  $D_{\text{H}_2\text{O}}$ , indicating the formation of strong intermolecular attractions between the two solvents. An increase in the OH site exchange rate from 0.98 to 7.95  $\text{s}^{-1}$  suggests that access of bulk water to polymer OH sites has increased significantly. The increase in water concentration should reduce the goodness of the solvent, but in this case the change in solvent quality must force a change in polymer conformation which allows increased access of bulk water to the water-bound OH sites. Minimizing interactions between the hydrophilic water-bound hydroxyl sites and the hydrophobic polymer backbone may drive the change in conformation. No change was detected in the  $R_{\text{H}}$  of the polymer, so the change in polymer conformation does not produce a significant expansion of the polymer chain.

**10K-20-21D after 6- and 12-month Storage Periods.** The significant increase in the OH site exchange rate after 6 months may be explained by a slow change in polymer conformation in response to a buildup of water around the OH sites. A further increase in  $D_{\text{DMSO}}$  and  $D_{\text{H}_2\text{O}}$  to values similar to the 10K-0 sample indicates a large proportion of the water is preferentially solvating the polymer at this stage. It is apparent from the broadening of the OH signal in the  $^1\text{H}$  spectra that the OH site mobility is reduced in the samples after 6 and 12 months. Combined with the increased exchange rate, the OH peak broadening indicates that the OH sites are strongly hydrated. The bound water is able to exchange rapidly with the bulk water, suggesting that the conformation adopted allows free access of water to all OH sites. There is an increase in  $R_{\text{H}}$  which is indicative of chain expansion; an increase in bound water around the hydroxyl sites, combined with hydrophobic hydration of the polymer backbone, forces the polymer chain into an extended conformation, and this increases the accessibility of the OH sites to the bulk water. The conformational change is revealed by the significantly increased OH exchange rate. This process occurs slowly with time; adding water to the 10K-20-21D sample may have accelerated the early stages of this transformation, since the exchange rate in 10K-60-21D was increased relative to 10K-20-21D, but not to the extent observed for 10K-20-21D after 6 or 12 months.

The 10K-60-21D sample was not stored, so no long-term data were available for this sample. As discussed above, the 10K-0 sample was kept and absorbed water during storage; a reduction in exchange rate would have been expected since the OH:H<sub>2</sub>O had increased from 1:5 to 1:30, but the OH exchange rate did not decrease significantly. This indicates that the sample has undergone some conformational transformation, and it is likely

**Table 5. Diffusion Coefficients and Molar Ratios of H<sub>2</sub>O:OH for 40.8K, 87K, and 230K PHEMA Solutions**

sample	$D_{\text{A}}$ ( $10^{-10} \text{ m}^2 \text{ s}^{-1}$ )	$D_{\text{B}}$ ( $10^{-11} \text{ m}^2 \text{ s}^{-1}$ )	OH:H <sub>2</sub> O integrated area (NMR)	OH (M)	H <sub>2</sub> O (M)	molar ratio H <sub>2</sub> O:OH
40.8K-0	8.1	2.4	1:2.5	0.077	0.096	1.25
40.8K-20-0D	7.72	2.24	1:40	0.077	1.54	20
40.8K-40-0D	7.28	2.11	1:68	0.077	2.62	34
40.8K-60-0D	7.16	2.05	1:115	0.077	4.43	57.5
87K-0	8.08	1.81	1:5	0.077	0.194	2.5
87K-20-0D	8.0	1.69	1:38	0.077	1.46	19
230K-0	8.06	1.1	1:2	0.077	0.154	2

that with time this sample would resemble the 10K-20-21D samples after 6- and 12-month storage periods. It seems likely that all samples of 10K PHEMA containing sufficient water would show similar time-dependent exchange behavior.

The conformational rearrangement of 10K PHEMA resulting from preferential solvation of the OH sites by water molecules could explain the changes observed in the exchange properties of 10K PHEMA in DMSO- $d_6$  upon addition of water both initially and over longer time periods. Initial conformational changes in response to added water are most likely due to a reduction in the goodness of the solvent. The number of water molecules associating with the OH sites increases over time and forces the polymer to adopt a conformation to minimize interactions between the hydrophilic water-bound OH sites and the hydrophobic polymer backbone. These changes in polymer conformation and the corresponding changes in access of the bulk water to the bound/slow diffusing water around the OH sites are reflected in the OH site exchange rate. Monitoring the exchange rate of the OH sites with water thus enables changes in polymer conformation to be detected using PFG-NMR. The concentration of bound water increases slowly over a period of months and results in an extended conformation where all polymer OH sites exchange rapidly with water, and the exchange rate is similar to the HEMA monomer. This appears to be a stable conformation; the only difference between the 10K-20-6M and 10K-20-12M samples was a broader OH signal in the  $^1\text{H}$  NMR spectra; exchange properties were identical, indicating the exchange rate had reached a maximum.

#### Exchange Properties of Higher MW Linear PHEMA.

Table 5 summarizes the diffusion coefficients and molar ratios of water to hydroxyl groups for PHEMA samples of MW 40 800, 87 000, and 230 000 in DMSO- $d_6$  solutions.

**40 800 MW PHEMA.** Logarithmic normalized hydroxyl signal intensities of 40.8K-0 and 40.8K-20-0D as a function of the squared gradient intensity are shown in Figure 6a,b. Similar to the situation with 10K PHEMA, the fastest exchange was observed in the sample with no added water. The 40.8K PHEMA also exhibited a significant reduction in exchange rate after the addition of 20  $\mu\text{L}$  water. In contrast to the 10K PHEMA, the effect of adding water was immediate; the experiment was conducted 2 h after preparing the sample, and the reduction in exchange was similar to the 10K sample after 21 days. The 40.8K PHEMA was monitored weekly for 6 weeks, and the exchange properties were invariant, indicating no further changes in the details of the interactions between the hydroxyl groups and water were occurring over time. After 12 months 40.8K-20-0D was checked, and the exchange properties had not changed; this suggests that the 40.8K PHEMA immediately forms a conformation with long-term stability. To assess the effect of adding further quantities of water to the 40.8K sample, 40  $\mu\text{L}$  of extra water was added in  $2 \times 20 \mu\text{L}$  increments. The diffusion decay data are shown in Figure 7. The experimental data were simulated as described for 10K PHEMA, and the simulations matched the experimental data closely. The estimates of  $k_B$  obtained graphically and from simulating the experimental data are shown in Table 6.

The exchange rate for 40.8K-0 is  $\sim 60\%$  less than observed for 10K-0; the number of exchanging sites is estimated to be 23% (relative to HEMA). The actual number of OH sites involved in exchange is quite low, indicating many of the OH sites have a reduced accessibility to water. A decrease in the mean value of  $k_B$  occurred upon addition of 20  $\mu\text{L}$  of water, followed by an increase after addition of a further 40  $\mu\text{L}$  of water. The estimated number of exchanging sites in this sample

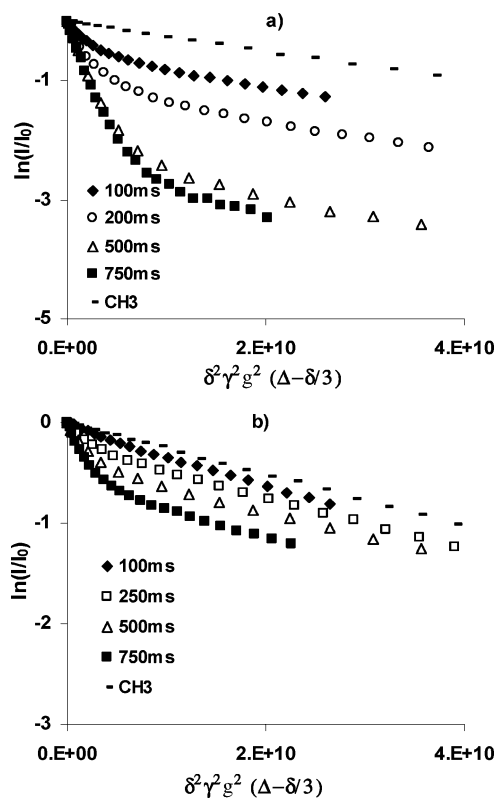


**Figure 6.** Logarithmic normalized OH signal intensity as a function of  $\gamma^2 \delta^2 g^2 (\Delta - \delta/3)$ : (a) 40.8K-0  $\Delta = 100-500$  ms; (b) 40.8K-20-0D  $\Delta = 100-750$  ms. CH<sub>3</sub>  $\Delta = 500$  ms shown to represent zero exchange in each plot.

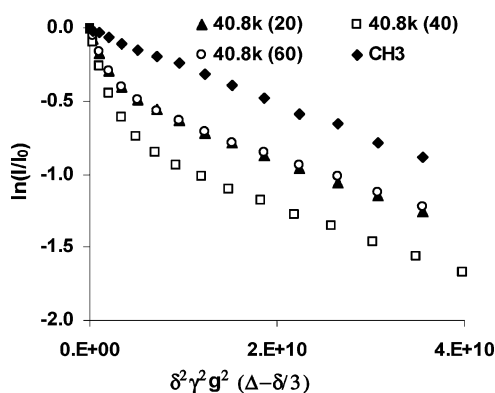


**Figure 7.** Logarithmic normalized OH signal intensity as a function of  $\gamma^2 \delta^2 g^2 (\Delta - \delta/3)$ : 40.8K-20-0D, 40.8K-40-0D, and 40.8K-60-0D. OH signal  $\Delta = 500$  ms, CH<sub>3</sub>  $\Delta = 500$  ms shown to represent zero exchange.

was  $<5\%$ . The increase in exchange rate observed is small when compared to that observed for 10K where the addition of 40  $\mu\text{L}$  of extra water produced a significant increase in hydroxyl group exchange. Adding a further 20  $\mu\text{L}$  to bring the total water added to 60  $\mu\text{L}$  resulted in  $k_B$  returning to a level of exchange similar to the sample containing 20  $\mu\text{L}$  of water. Only slight changes in the exchange rates were observed with time; even after 12 months the 40.8K-60-0D sample exchange rate had only increased from 1.05 to 1.75  $\text{s}^{-1}$  (Table 6).

On the basis of the reduction in OH exchange rate relative to 10K PHEMA, it can be concluded that the 40.8K PHEMA chain must adopt a more compact conformation in solution. An equivalent number of hydroxyl sites are present in all polymer solutions (0.077 M), so differences in exchange rates can be viewed as molecular weight dependent conformation changes.

**Table 6. Comparison of  $k_B$  Values and % Exchanging Sites Obtained Using Graphical Analysis and Simulations for 40.8K, 87K, and 230K PHEMA Samples**

	sample	$k_B$ ( $s^{-1}$ ) graph	$k_B$ ( $s^{-1}$ ) simulation	$k_B$ ( $s^{-1}$ ) mean	$\tau_B$ (s) mean	% exchanging OH sites	molar ratio H <sub>2</sub> O:OH
1	40.8K-0	4	6.3	5.2	0.19	23	1.25
2	40.8K-20-0D	0.76	0.9	0.83	1.2	3.4	20
3	40.8K-20-42D	0.85	1.2	1.03	0.97	4.1	21.5
4	40.8K-40-0D	1.49	1.4	1.45	0.69	6.4	34
5	40.8K-40-21D	1.4	1.1	1.25	0.8	5	35
6	40.8K-60-0D	1.1	1	1.05	0.95	4.2	57.5
7	40.8K-60-12M	1.5	2	1.75	0.57	7	70
8	87K-0	6	7.5	6.75	0.148	30	2
9	87K-20-0D	0.32	0.3	0.31	3.2	1.4	19
10	230K-0	0.74	1	0.87	1.15	3.9	1.1

**Table 7. Diffusion Coefficients of Residual DMSO in DMSO- $d_6$  and Water in 40.8K PHEMA Samples**

sample	$D_{DMSO}$ ( $10^{-10}$ m <sup>2</sup> s <sup>-1</sup> )	$D_{H_2O}$ ( $10^{-10}$ m <sup>2</sup> s <sup>-1</sup> )
40.8K-0	6.36	8.1
40.8K-20-0D	6.0	7.72
40.8K-20-42D	6.0	7.8
40.8K-20-12M	5.86	7.61
40.8K-40-0D	5.7	7.28
40.8K-40-21D	5.64	7.42
40.8K-60-0D	5.3	7.16
40.8K-60-12M	5.35	7.08

If the 40.8K PHEMA adopts a more compact coil conformation in which polymer–polymer interactions are strong, and therefore hydration of the OH sites is low, a reduction in the OH exchange rate is expected.

The diffusion coefficients for DMSO- $d_6$  and water in the 40.8K PHEMA solutions are shown in Table 7. In contrast to the 10K PHEMA samples, it is apparent that  $D_{DMSO}$  and  $D_{H_2O}$  do not show time-dependent changes. This is reasonable, since the 40.8K PHEMA samples do not show any significant time-dependent changes in OH exchange rates; the samples equilibrate quickly and remain stable for long periods. Preferential hydration of the OH sites is not extensive, and the composition of the solvent remains constant as illustrated by the diffusion coefficients in Table 7. The changes in OH exchange rate observed upon addition of water most likely involve conformational changes in response to the solvent goodness. The changes in exchange rate with addition of water reflect the change in polymer conformation in response to a reduction in the goodness of the solvent. The polymer will adopt the most stable conformation possible for a particular solvent composition. The conformation adopted in order to minimize interactions between OH sites with bound water and the hydrophobic polymer backbone allows increased access of bulk water to the water-bound OH sites, and an increase in the rate of exchange is observed.

**87 000 and 230 000 MW PHEMA.** The estimates of  $k_B$  obtained graphically and from simulating the experimental data for these polymers in solution are shown in Table 6; similar to the 10K and 40.8K PHEMA samples, the simulations matched the experimental data closely. The 87K-0 and 87K-20-0D samples exhibited very similar exchange behavior to the 40.8K-0 and 40.8K-20-0D samples. The exchange properties of the 87K-0 and 87K-20-0D remained stable from the time of preparation and over a period of months. The similar exchange behavior suggests the 40.8K and 87K polymers adopt similar conformations in solution. The largest polymer used in this study had a MW of  $\sim 230$ K from  $^1H$  NMR—the estimate may contain a significant error as it is reliant on integration of a very small end-group signal. The Steskjal–Tanner plots comparing 10K, 40.8K, 87K, and 230K linear PHEMA samples with no water added for  $\Delta = 500$  ms are compared in Figure 8. The exchange

rate of the 230K-0 sample was very slow compared with the lower MW polymers, suggesting a very compact conformation where very few OH sites are solvent accessible.

**Scaling Law.** The dependence of the diffusion coefficient on the polymer molar mass can be described by a scaling relation:

$$D \sim M_n^\alpha$$

$D$  is the diffusion coefficient,  $M$  is the number-average MW, and  $\alpha$  is a scaling constant. The scaling constant  $\alpha$  is predicted to be between  $-0.6$  and  $-0.5$  for a fully solvated polymer chain in a good solvent and  $-0.33$  for a collapsed polymer chain.<sup>31,32</sup> A fully solvated chain occurs in a solvent when the polymer–solvent interactions predominate over polymer–polymer interactions; a collapsed chain occurs in a poor solvent where polymer–polymer interactions dominate.

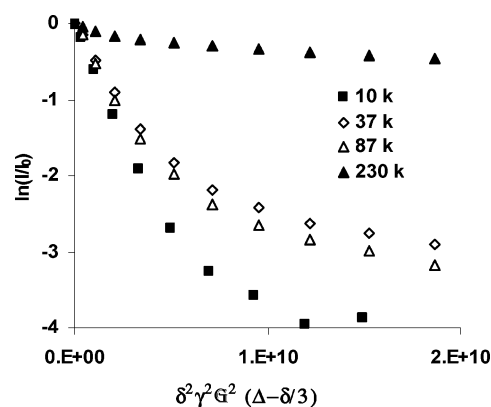
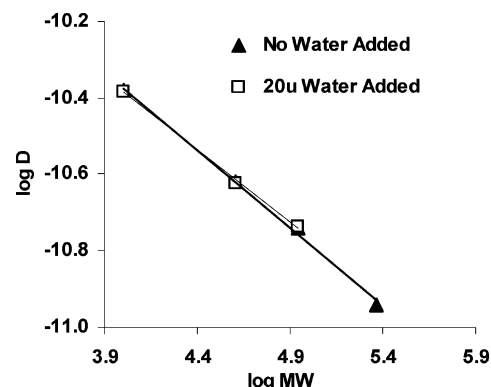
**Figure 8.** Logarithmic normalized OH signal intensity as a function of  $\gamma^2\delta^2g^2(\Delta - \delta/3)$ : 10K-0, 40.8K-0, 87K-0, and 230K-0 samples  $\Delta = 500$  ms.**Figure 9.** Dependence of self-diffusion on molar mass for linear PHEMA of 10K, 40.8K, 87K, and 230K. Data for no added water and 20  $\mu$ L of added water are shown.



Figure 9 shows a plot of  $\log D_{\text{CH}_3}$  vs  $\log \text{MW}$  for the 10K, 40.8K, and 87K-0 samples and 10K, 40.8K, and 87K-20-0D samples; it is clear that  $D_{\text{CH}_3}$  follows a scaling law. The value of the slope obtained from linear regression provided  $\alpha$  values for the exponent in the scaling law of  $-0.41$  and  $-0.38$  for the 0 and 20  $\mu\text{L}$  of added water cases, respectively. DMSO is therefore a poor (worse than  $\theta$  for which  $\alpha = -0.5$ ) solvent for PHEMA, and the addition of water further reduces the goodness of the solvent; the polymer chains must exist in a compact, almost collapsed state. This may explain why larger changes in  $R_H$  are not observed in the 10K PHEMA samples even though the exchange properties vary significantly compared with the larger MW PHEMA.

## Conclusions

PFG-NMR has been applied to study chemical exchange rates of OH sites on linear PHEMA of MW 10 000–230 000 in DMSO- $d_6$  containing varying quantities of water. The experimental data were simulated closely for the two-site exchange case using the Bloch equations modified for the effects of chemical exchange and diffusion. The exchange rate could be used to detect both subtle changes in polymer conformation resulting from changes in the solvent and MW-dependent conformational differences. Linear PHEMA of MW 10K showed significant time-dependent changes in exchange rate resulting from preferential solvation of the OH sites by water and subsequent conformational changes which altered accessibility of the OH sites to water. A significant increase in exchange rate was observed with time for 10K PHEMA with added water. This behavior was not observed for larger MW PHEMA; these samples exhibited much lower exchange rates than the 10K PHEMA and did not change as a function of time. An equivalent number of hydroxyl sites were present in all polymer solutions, so differences in exchange rates were attributed to molecular weight dependent conformation changes. Access of water to OH sites on larger polymers was hindered and became most hindered in the largest PHEMA studied. Only small changes in hydrodynamic radius were observed for most samples, even with large changes in OH site exchange rates. This suggests that a change in the accessibility of the OH sites involves relatively small changes in chain conformation or that rearrangements can occur with minimal overall change in the chain dimensions. DMSO was found to be a poor solvent for PHEMA, and the addition of water further reduced the goodness of the solvent; PHEMA therefore exists in a compact, almost collapsed state in DMSO. It has been demonstrated that the use of PFG-NMR for the measurement of chemical exchange rates

is a powerful technique for detecting subtle changes in polymer conformation in polymers with exchangeable protons, in addition to providing a diffusion coefficient for the polymer. Experiments take only 20–30 min depending on sample concentration and provide an abundance of information in one experiment.

## References and Notes

- (1) Johnson, C. S. *Prog. Nucl. Magn. Reson. Spectrosc.* **1999**, *34*, 203.
- (2) Jerschow, A.; Muller, N. *Macromolecules* **1998**, *31*, 6573–6578.
- (3) Chen, A.; Shapiro, M. J. *Anal. Chem.* **1999**, *71*, 669A.
- (4) Morris, K. F.; Johnson, C. S. *J. Am. Chem. Soc.* **1993**, *115*, 4291–4299.
- (5) Dempsey, C. *Prog. Nucl. Magn. Reson. Spectrosc.* **2001**, *39*, 135.
- (6) Perrin, C. L.; Dwyer, T. J. *Chem. Rev.* **1990**, *90*, 935–967.
- (7) Tonelli, A. E.; Srinivasarao, M. *Polymers from the Inside Out—An Introduction to Macromolecules*; Wiley-Interscience: New York, 2001.
- (8) Cabrita, E. J.; Berger, S.; Brauer, P.; Karger, J. J. *Magn. Reson.* **2002**, *157*, 124–131.
- (9) Moonen, C. T. W.; van Gelderen, P.; Vuister, W.; van Zijl, P. C. M. *J. Magn. Reson.* **1992**, *97*, 419–425.
- (10) Johnson, C. S. *J. Magn. Reson.* **1993**, *102*, 214–218.
- (11) Xu, B.; Lynn, G. W.; Guo, G.; Melnichenko, Y. B.; Wignall, G. D.; McClain, J. B.; DeSimone, J. M.; Johnson, C. S. *J. Phys. Chem. B* **2005**, *109*, 10261–10269.
- (12) Kang, S. K.; Jhon, M. S. *J. Polym. Sci., Part A* **1991**, *29*, 393–398.
- (13) Barbieri, R.; Quaglia, M.; Delfini, M.; Brosio, E. *Polymer* **1998**, *39*, 1059–1066.
- (14) Wichterle, O.; Lim, D. *Nature (London)* **1960**, *185*, 117–118.
- (15) Jerschow, A.; Muller, N. *J. Magn. Reson.* **1997**, *125*, 372–375.
- (16) Price, W. S. *Concepts Magn. Reson.* **1997**, *9*, 299–336.
- (17) Waldeck, A. R.; Kuchel, P. W.; Lennor, A. J.; Chapman, B. E. *Prog. Nucl. Magn. Reson. Spectrosc.* **1997**, *30*, 39–68.
- (18) Hoffman, A. S. *Adv. Drug Delivery Rev.* **2002**, *43*, 3–12.
- (19) Capitani, D.; Crescenzi, V.; De Angelis, A. A.; Segre, A. L. *Macromolecules* **2001**, *34*, 4136–4144.
- (20) Whittaker, A.; Ghi, P.; Hill, D.; Whittaker, M. *Polym. Mater. Sci. Eng.* **1998**, *79*, 467–468.
- (21) Branca, C.; Magazu, S.; Maisano, G.; Migliardo, P.; Tettamanti, E. *Physica B* **2000**, *291*, 180–189.
- (22) Maeda, K.; Morino, K.; Yashima, E. *J. Polym. Sci., Part A* **2003**, *41*, 3625–3631.
- (23) Porcar, I.; Solar, L.; Abad, C.; Gomez, C. M.; Campos, A. J. *Chromatogr. A* **2004**, *1031*, 117–123.
- (24) Khatri, C. A.; Pavlova, Y.; Green, M. M.; Morawetz, H. *J. Am. Chem. Soc.* **1997**, *119*, 6991–6995.
- (25) Young, T. H.; Chuang, W. Y. *J. Membr. Sci.* **2002**, *210*, 349–359.
- (26) Geerke, D. P.; Oostenbrink, C.; van der Vegt, N.; van Gunsteren, W. F. *J. Phys. Chem. B* **2004**, *108*, 1436–1445.
- (27) Kang, S. K.; Jhon, M. S. *J. Polym. Sci., Part A* **1993**, *31*, 1243–1251.
- (28) Ghi, P.; Hill, D. J. T.; Whittaker, A. K. *J. Polym. Sci., Part B* **2000**, *38*, 1939–1946.
- (29) Wang, X.; Qiu, X.; Wu, C. *Macromolecules* **1998**, *31*, 2972–2976.
- (30) Chowdhuri, S.; Chandra, A. J. *Chem. Phys.* **2003**, *119*, 4360–4366.
- (31) Wilkins, D. K.; Grimshaw, S. B.; Receveur, V.; Dobson, C. M.; Jones, J. A.; Smith, L. J. *Biochemistry* **1999**, *38*, 16424–16431.
- (32) Zhao, T.; Beckham, H. W. *Macromolecules* **2003**, *36*, 9859–9865.

MA0603550